

1 **Reviewer 1#**

2 This is an interesting study, using machine learning to estimate the ozone formation
3 sensitivity. The idea is not novel (a few previous studies with similar scope are cited in
4 this manuscript). The method, using reactivity-corrected VOC measurements (i.e.,
5 initial VOC concentrations), sheds some insights into ozone production in an urban
6 environment.

7 **Reply:** Thanks for your positive comments. We have carefully responded to all of your
8 **point-by-point** comments and issues and have revised the manuscript accordingly.
9 These revisions are described in detail below.

10

11 However, there are several major issues:

12 **Q1:** (1) The machine learning workflow described in this manuscript does not include
13 a robust or systematic solution to mitigate overtraining. I will elaborate on this later but
14 the measures described in this work absolutely do not guarantee that overtraining is/can
15 be avoided.

16 **Reply:** Thank you for your good suggestion. According to your suggestion, we
17 performed a 12-fold cross-validation after data-normalization, i.e., by randomly
18 dividing the dataset into 12 subsets and alternately taking one subset as testing data and
19 the rest as training data. By doing this, every data point has an equal chance being
20 trained and tested. In lines 148-153 in the revised manuscript, we added a short
21 paragraph “To avoid over-fitting, we trained the random forest model using cross-
22 validation for the normalized data, which can improve the robustness of the model.
23 Briefly, we randomly divided the normalized data into 12 subsets, then alternately took
24 one subset as testing data along with the rest as training data. By doing this, every data
25 point has an equal chance being trained and tested.”.

26 We added the RF model workflow to Text S3 in the revised Supporting
27 Information.

28 **“Text S3. Workflow of RF model and the calculation of Relative Importance (RI)**
29 **The workflow of RF model used in this study was established through the following**
30 **steps.**

31 (1) Data description. The length of the input data from 2014 to 2016 were 1190, 1062
32 and 872 rows, respectively, in which different types of VOCs, NO_x, CO, PM_{2.5} and
33 meteorological parameters (including temperature, relative humidity, solar radiation,
34 wind speed and direction) were used as input variables and O₃ was the output variable.
35 The mean values (\pm standard deviation) of input/output parameters are shown in Table
36 S1.

37 (2) Data process. After the extreme values were removed, all data were normalized
38 (between 0 and 1) in order to decrease the sample distribution range, accelerate
39 calculation efficiency and improve the robustness of the RF model. Then, the dataset
40 was randomly divided into 12 subsets. Thus, a 12-fold cross-validation was performed
41 by alternately taking one subset as testing data and the rest as training data to ensure
42 that each data point has an equal chance being trained and tested.

43 (3) Hyper-parameters optimization. All network configuration parameters (i.e., leaf
44 number, number of trees, algorithm, and so on) were modified by a trial and error
45 method to obtain the optimized network structure. The optimized RF model parameters
46 are shown in Table S2. Figures S13 and S14 show the examples to optimize the number
47 of minimal samples split and trees, respectively.

48 (4) Model uncertainty estimation. The uncertainty of the model was estimated
49 according to the predicted and observed O₃ concentrations. The performance of the
50 model was evaluated using R square (R^2) and Root Mean Squared Error (RMSE).

51 (5) Relative importance (RI) calculation: The influence of an input variable on model
52 performance was evaluated by changes in the accuracy of the model by variable
53 permuting. Briefly, a change of prediction error was resulted from permuting a variable
54 across the observations. The magnitude of the response was estimated using out-of-bag
55 error of a predictor according to following steps.

56 For a random forest model that has T learners and p predictors in the training data,
57 the first step is to identify the out-of-bag observations and the indices of the predictor
58 variables that are split to a growing tree t (from 1 to T). Then, one can estimate the out-
59 of-bag error (ϵ_t) for each tree. For a predictor variable x_j (j: from 1 to p), one can estimate
60 the model error ($\epsilon_{t,j}$) again corrodng to the out-of-bag observations after randomly

61 permuting the observations of x_j . Thus, the difference of the model error ($d_{t,j} = \varepsilon_{t,j} - \varepsilon_t$)
62 is obtained. If the predictor variables are not split, the difference of a growing tree t is
63 0. The second step is to calculate the mean difference of the model errors (\bar{d}_j), and the
64 standard deviation (σ_j) of the differences for all the learners and each predictor variable
65 in the training data. Finally, the out-of-bag relative importance (RI) for x_j is calculated
66 by dividing the difference of the model errors by the standard deviation (\bar{d}_j/σ_j).

67 (6) EKMA curves. The Empirical Kinetic Modeling Approach (EKMA) was used to
68 assess the O_3 formation mechanism regime. Both the RF model and a box model with
69 Master Chemical Mechanism (MCM, 3.3.1) were used to calculate the EKMA curves.
70 For the RF model simulations, the observed point data was chosen as the mean values
71 of the input parameters during our observations, then the concentrations of VOCs and
72 NO_x were varied $\pm 10\%$ (or from 90% to 110%) of their mean values with a step of 1%
73 in a two-dimensional matrix along with other inputs unchanged. This matrix was used
74 as the testing data, while all the measured data were taken as the training data in the RF
75 model to simulate O_3 concentrations under different scenarios of VOCs and NO_x
76 concentrations. To decrease the model uncertainty, we set relatively small variations of
77 VOCs and NO_x ($\pm 10\%$) compared to the observed values in this study. The mean
78 relative error of simulated O_3 concentrations between RF model and Box model (within
79 15.6%, Figure S8) suggests that the RF model can well predict O_3 concentrations during
80 our observations.”

81

82 **Q2:** (2) Random forest depends heavily on the training dataset. The authors do not
83 provide an overview of the comprehensiveness of the training dataset: for instance, does
84 the dataset cover all major chemical regimes in the EKMA plot, i.e., NO_x -limited,
85 VOC-limited, NO titration? The authors claim that ozone production in Beijing, China
86 is mostly VOC-limited, which is consistent with previous studies. If the training set
87 collected in Beijing does not have sufficient coverage in the NO_x -limited regime, then
88 the trained algorithm essentially attempts to extrapolate in that regime, which is
89 dangerous and prone to overtraining. I would then question the if this random forest

90 model can make meaningful forecast in that regime at all.

91 **Reply:** Thank you for your valuable suggestion. We added the description of training
 92 dataset in Text S3 in the revised SI. This point has been replied in the aforementioned
 93 question. The mean values (\pm standard deviation) of the input and output parameters for
 94 the training data set are shown in Table R1. This Table was also added as Table S1 in
 95 the revised SI.

96 **Table R1. An overview of training dataset from 2014 to 2016 during the observation**
 97 **period.**

species / unit	2014				2015				2016			
	Measured VOC		Initial VOC		Measured VOC		Initial VOC		Measured VOC		Initial VOC	
	aver age	std. dev.*	aver age	std. dev.	aver age	std. dev.	aver age	std. dev.	aver age	std. dev.	aver age	std. dev.
Cyclopentane / ppbv	0.95	1.05	0.95	1.05	0.00	0.00	0.00	0.00	0.27	0.29	0.27	0.29
Ethane / ppbv	2.38	0.98	2.39	0.98	1.84	0.88	1.85	0.89	1.07	0.51	1.07	0.51
Acetylene / ppbv	1.64	1.31	1.65	1.31	0.13	0.33	0.14	0.33	0.32	0.30	0.32	0.30
Propane / ppbv	2.44	1.60	2.46	1.61	2.42	1.75	2.45	1.76	1.35	0.93	1.36	0.93
Benzene / ppbv	0.60	0.44	0.61	0.44	0.47	0.35	0.47	0.36	4.59	4.23	4.64	4.29
iso-Butane / ppbv	0.95	0.66	0.96	0.67	0.35	0.53	0.35	0.54	0.24	0.18	0.24	0.19
2,2-Dimethylbutane / ppbv	0.00	0.01	0.00	0.01	0.00	0.02	0.00	0.02	0.00	0.00	0.00	0.00
n-Butane / ppbv	1.57	1.11	1.60	1.11	0.67	0.87	0.69	0.89	0.85	0.73	0.87	0.74
2,2,4-Trimethylpentane / ppbv	0.01	0.04	0.01	0.04	0.04	0.07	0.05	0.07	0.02	0.02	0.02	0.02
iso-Pentane / ppbv	0.11	0.38	0.11	0.40	0.00	0.00	0.00	0.00	0.16	0.18	0.16	0.18
2,3-Dimethylpentane / ppbv	0.07	0.08	0.07	0.08	0.06	0.08	0.06	0.08	0.02	0.03	0.02	0.03
3-Methylhexane / ppbv	0.06	0.07	0.06	0.07	0.04	0.05	0.04	0.05	0.01	0.02	0.01	0.02
Toluene / ppbv	1.28	1.02	1.32	1.04	0.88	1.55	0.93	1.57	0.30	0.34	0.32	0.37
2,3-Dimethylbutane / ppbv	0.00	0.00	0.00	0.00	0.00	0.03	0.00	0.03	0.06	0.08	0.06	0.08
n-Propyl benzene / ppbv	0.01	0.02	0.01	0.02	0.01	0.03	0.01	0.03	0.04	0.11	0.05	0.11

iso-Propyl benzene / ppbv	0.00	0.01	0.00	0.01	0.00	0.00	0.00	0.00	0.01	0.05	0.01	0.06
2,3,4- trimethylpentane / ppbv	0.12	0.29	0.12	0.31	0.06	0.10	0.06	0.11	0.01	0.02	0.02	0.02
n-hexane / ppbv	0.37	0.30	0.39	0.31	0.05	0.18	0.06	0.20	0.18	0.27	0.19	0.30
n-heptane / ppbv	0.08	0.09	0.09	0.10	0.06	0.06	0.06	0.07	0.02	0.02	0.02	0.02
2-methylhexane / ppbv	0.03	0.03	0.03	0.04	0.02	0.04	0.02	0.04	0.01	0.01	0.01	0.01
3-methylhexane / ppbv	0.01	0.02	0.01	0.02	0.01	0.02	0.01	0.02	0.00	0.01	0.00	0.01
cyclohexane / ppbv	0.04	0.05	0.05	0.05	0.03	0.05	0.04	0.05	0.04	0.10	0.04	0.12
ethylbenzene / ppbv	0.33	0.31	0.34	0.32	0.21	0.23	0.23	0.25	0.10	0.15	0.10	0.16
n-octane / ppbv	0.04	0.11	0.04	0.11	0.00	0.00	0.00	0.00	0.00	0.00	0.00	0.00
ethene / ppbv	2.15	1.36	2.31	1.43	1.72	1.16	1.90	1.25	0.39	0.30	0.41	0.31
methylcyclohexa ne / ppbv	0.01	0.03	0.01	0.03	0.01	0.03	0.01	0.04	0.02	0.03	0.02	0.04
n-nonane / ppbv	0.03	0.04	0.03	0.04	0.02	0.02	0.02	0.03	0.02	0.04	0.02	0.04
n-decane / ppbv	0.02	0.04	0.02	0.05	0.02	0.03	0.02	0.03	0.00	0.01	0.00	0.01
p-ethyltoluene / ppbv	0.06	0.08	0.06	0.08	0.02	0.03	0.03	0.04	0.07	0.10	0.07	0.11
p-diethyl benzene / ppbv	0.01	0.04	0.01	0.04	0.01	0.02	0.01	0.02	0.09	0.17	0.11	0.22
o-ethyl toluene / ppbv	0.03	0.04	0.04	0.04	0.01	0.03	0.01	0.03	0.08	0.28	0.09	0.32
o-xylene / ppbv	0.09	0.18	0.10	0.18	0.16	0.18	0.19	0.20	0.14	0.26	0.15	0.27
m-ethyl toluene / ppbv	0.02	0.07	0.02	0.07	0.04	0.09	0.04	0.09	0.03	0.04	0.03	0.05
m-diethyl benzene / ppbv	0.01	0.03	0.01	0.03	0.00	0.01	0.00	0.01	0.00	0.02	0.00	0.02
m/p-Xylene / ppbv	0.61	0.64	0.68	0.65	0.45	0.51	0.54	0.59	0.22	0.38	0.25	0.41
propene / ppbv	2.07	1.18	2.83	2.26	4.40	2.61	6.60	6.12	0.28	0.41	0.34	0.45
1-Butene / ppbv	0.10	0.14	0.13	0.17	0.04	0.10	0.08	0.25	0.03	0.03	0.04	0.06
1-Pentene / ppbv	0.03	0.09	0.04	0.09	0.03	0.07	0.05	0.12	0.02	0.06	0.02	0.07
1,2,4-trimethyl benzene/ ppbv	0.01	0.08	0.01	0.08	0.08	0.09	0.11	0.12	0.05	0.05	0.06	0.09
1,2,3-trimethyl benzene/ ppbv	0.00	0.01	0.00	0.01	0.03	0.05	0.04	0.08	0.05	0.28	0.05	0.28
a-pinene / ppbv	0.01	0.03	0.02	0.03	0.01	0.03	0.01	0.03	0.18	0.46	0.84	3.48
cis-2-Butene / ppbv	0.34	0.70	0.85	2.67	0.66	0.85	1.77	4.56	0.04	0.05	0.11	0.29

1,3,5-Trimethylbenzene / ppbv	0.05	0.07	0.08	0.11	0.03	0.05	0.07	0.14	0.25	0.56	1.07	4.11
styrene / ppbv	0.18	0.27	0.30	0.61	0.00	0.03	0.01	0.08	0.27	0.79	0.57	2.08
2-methyl-1-pentene / ppbv	0.18	0.37	0.72	2.94	0.04	0.04	0.26	1.68	0.02	0.09	0.03	0.12
trans-2-Butene / ppbv	0.08	0.16	0.24	1.15	0.09	0.11	0.34	0.74	0.02	0.02	0.04	0.08
cis-2-Pentene / ppbv	0.15	0.20	0.37	0.93	0.17	0.17	0.91	4.24	0.01	0.02	0.02	0.08
1,3-Butadiene / ppbv	0.09	0.10	0.19	0.34	0.04	0.05	0.12	0.38	0.02	0.03	0.05	0.25
trans-2-Pentene / ppbv	0.03	0.08	0.06	0.27	0.01	0.02	0.11	0.89	0.01	0.02	0.01	0.05
β -pinene / ppbv	0.00	0.01	0.01	0.03	0.01	0.01	0.02	0.15	0.00	0.01	0.00	0.02
isoprene / ppbv	0.89	0.64	5.70	18.7	0.34	0.43	6.40	21.5	0.13	0.17	2.12	7.46
NO / ppbv	7.03	17.02	7.03	17.0	3.38	5.59	3.38	5.59	5.28	10.3	5.28	10.3
NO ₂ / ppbv	15.5	15.79	15.5	15.7	19.1	12.6	19.1	12.6	18.7	12.4	18.7	12.4
T / ° C	22.5	6.28	22.5	6.28	22.7	5.24	22.7	5.24	22.3	4.85	22.3	4.85
RH / %	50.9	23.88	50.9	23.8	41.4	23.2	41.4	23.2	36.2	21.5	36.2	21.5
SR / W m ⁻²	162.	222.9	162.	222.	153.	205.	153.	205.	150.	199.	150.	199.
WS / m s ⁻¹	3.11	2.70	3.11	2.70	2.29	2.15	2.29	2.15	1.25	1.24	1.25	1.24
WD / °	162.	105.0	162.	105.	175.	101.	175.	101.	184.	108.	184.	108.
PM _{2.5} / $\mu\text{g m}^{-3}$	67.1	53.47	67.1	53.4	63.1	56.4	63.1	56.4	61.0	48.6	61.0	48.6
CO / mg m ⁻³	0.78	0.49	0.78	0.49	0.68	0.44	0.68	0.44	0.57	0.36	0.57	0.36
O ₃ / ppbv	44.3	32.38	44.3	32.3	42.7	27.9	42.7	27.9	44.0	29.6	44.0	29.6

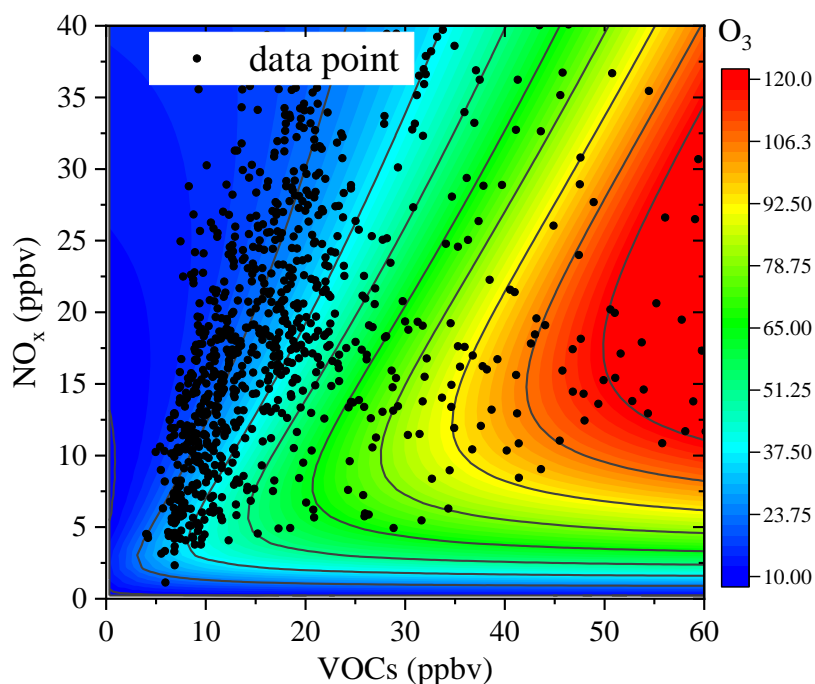
98 * Standard Deviation (std. Dev.)

99

100 In Text S3 in the revised SI, we added a short paragraph “Data description. The
101 length of the input data from 2014 to 2016 were 1190, 1062 and 872 rows, respectively,
102 in which different types of VOCs, NO_x, CO, PM_{2.5} and meteorological parameters
103 (including temperature, relative humidity, solar radiation, wind speed and direction)

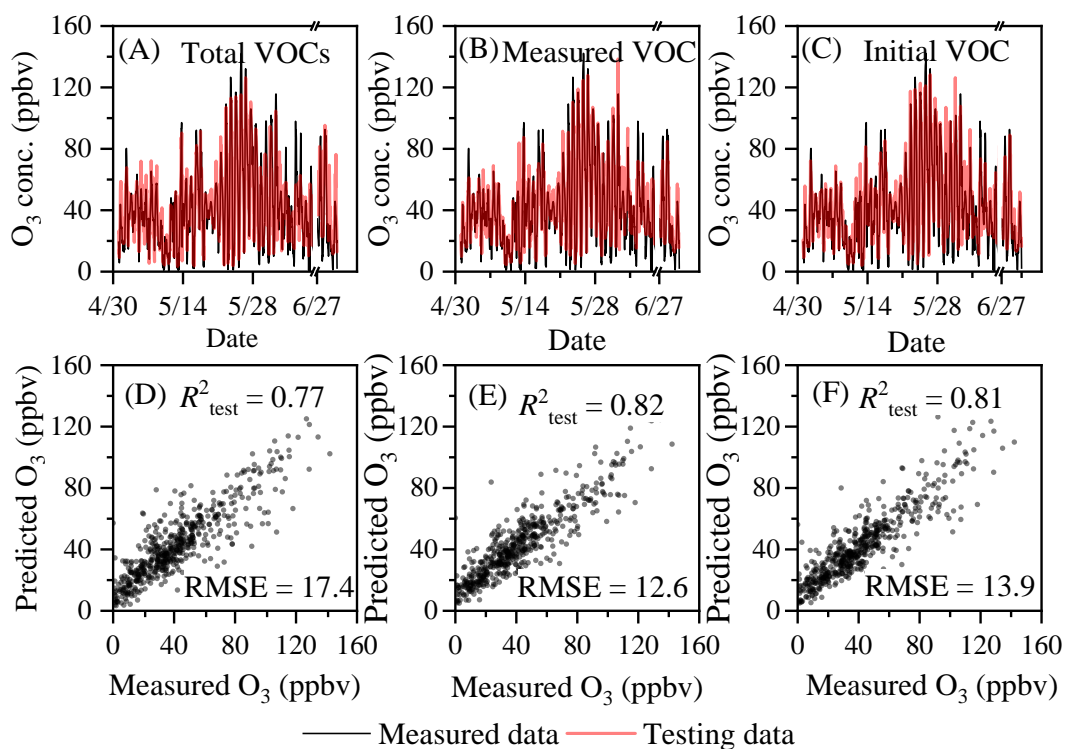
104 were used as input variables and O₃ was the output variable. The mean values
105 (\pm standard deviation) of input/output parameters are shown in Table S1”

106 As shown in Figure R1 or Figure S15, the training dataset were located in VOC-
107 limited, NO_x-limited, and transition regimes, while most of the training data were
108 located in the VOC-limited regime. To avoid overtraining, we performed a 12-fold
109 cross-validation, i.e., by randomly dividing the observed data into 12 subsets and
110 alternately taking one subset as testing data and the rest as training data, to ensure that
111 each data point has an equal chance of being trained and tested. Figure R2 (Figure 2 in
112 the revised manuscript) shows the comparisons between the measured and predicted O₃
113 concentrations using different VOC inputs. The curves of the predicted O₃
114 concentrations were spliced using the testing datasets in all runs. Thus, both the training
115 data and the testing data actually covered all the sensitivity regimes of O₃ formation.
116 We think that the model is robust in the revised version according to your good
117 suggestion.



118

119 **Figure R1.** Sensitivity curves of O₃ formation and distribution of training data in 2015.



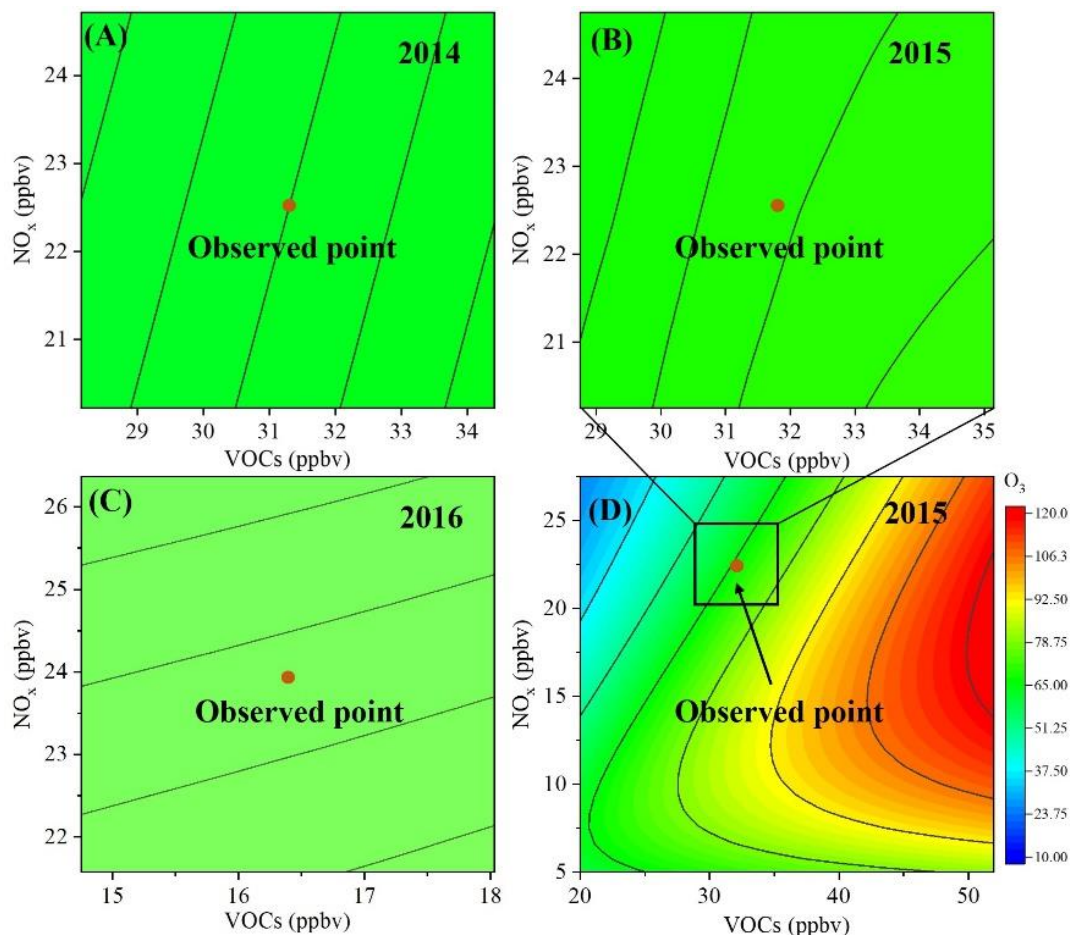
120

121 **Figure R2.** Comparison of the predicted and measured O₃ concentrations in Beijing in
 122 the summer of 2015. (A and D: TVOC concentrations; B and E: measured
 123 concentrations of VOC species; C and F: initial concentrations of VOC species). The
 124 testing data curves were spliced using the testing datasets in all runs during the 12-fold
 125 cross-validation.

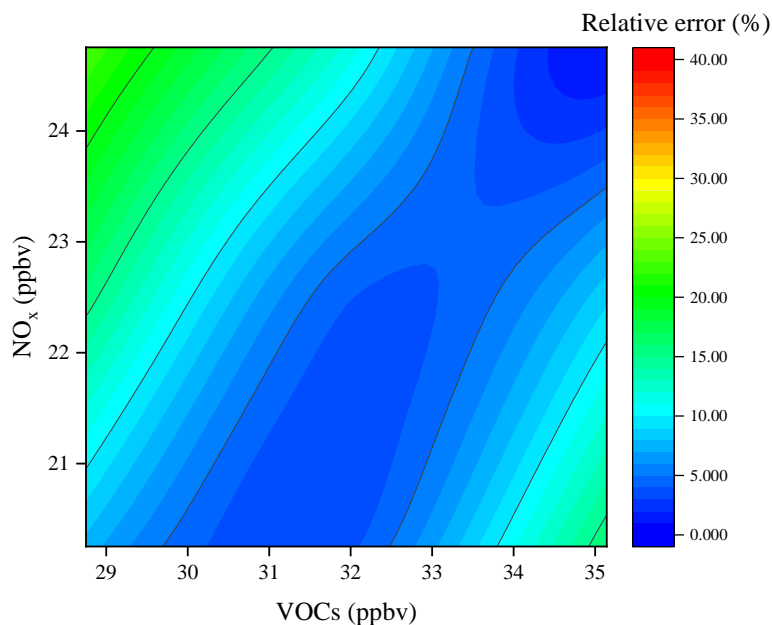
126

127 When plotting the O₃ formation sensitivity curves, we made a virtual matrix of
 128 inputs by varying the concentrations of NO_x and VOCs from 0.9 to 1.1 times (with a
 129 step of 0.01) of their mean values (observed point data) while keeping all other inputs
 130 unchanged (i.e., the mean values during our observations). Then, the new matrix was
 131 used as testing data, while all the measured data were taken as training data. Thus, the
 132 testing data should represent the mean sensitivity regime of O₃ in Beijing, while the
 133 training data actually covered all the sensitivity regimes of O₃ formation. As shown in
 134 Figure R3 or Figure 4B, the sensitivity of O₃ formation was located in VOC-limited
 135 regime in 2015. The mean relative errors of simulated O₃ between RF model and Box
 136 model was 15.6% (Figure R4 or Figure S8), which means that the RF model can well
 137 predict the O₃ concentrations and the sensitivity regime of O₃ formation. Although we

138 set relatively small variations of VOCs and NO_x ($\pm 10\%$) compared to the observed
139 values to decrease the model uncertainty when depicting the EKMA curves, the training
140 data represent the real conditions in Beijing during our observations. Therefore, we
141 think our results should be reliable and meaningful.



142
143 **Figure R3.** Ozone formation sensitivity curves from 2014-2016. (A, B, C: calculated
144 by the RF model for 2014, 2015, and 2016, respectively. D: calculated by the OBM for
145 2015)



146

147 **Figure R4.** The relative error of simulated O₃ concentrations between the RF model
 148 and the box model in 2015.

149 In lines 232-240 the revised manuscript, we added a paragraph “It should be
 150 pointed out that if the training dataset does not have sufficient coverage in the NO_x-
 151 limited regime, then the trained algorithm essentially attempts to extrapolate in that
 152 regime, which is prone to overtraining. To avoid such overtraining, a 12-fold cross-
 153 validation by randomly dividing the observation data in each day into 12 subsets and
 154 alternately taking one subset as testing data and the rest as training data ensures that
 155 each data point has an equal chance of being trained and tested. The curves of the
 156 predicted O₃ concentrations in Figure 2 were spliced using the testing datasets in all
 157 runs. Thus, our results actually covered all the sensitivity regimes of O₃ formation. This
 158 means that the model is robust”.

159 In lines 171-178 in the revised manuscript, we added a paragraph “When plotting
 160 the O₃ formation sensitivity curves, we made a virtual matrix of inputs by varying the
 161 concentrations of NO_x and VOCs from 0.9 to 1.1 times (with a step of 0.01) of their
 162 mean values while keeping all other inputs unchanged (i.e., the mean values). Then, the
 163 new matrix was used as testing data, while all the measured data were taken as training
 164 data. Thus, the testing data should represent the mean sensitivity regime of O₃ in Beijing,
 165 while the training data actually covered all the sensitivity regimes of O₃ formation to

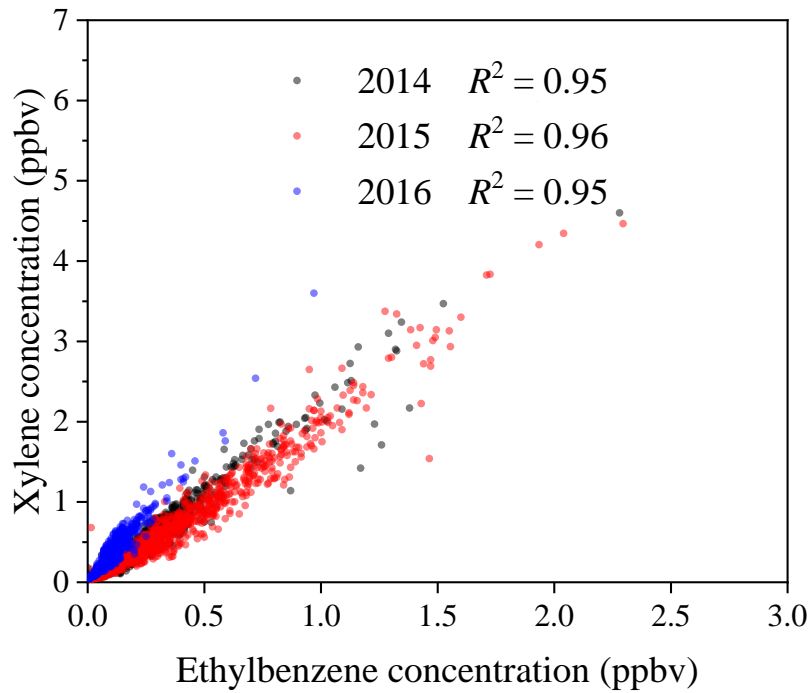
166 guarantee a sufficient coverage in the NO_x-limited regime for the RF model
167 simulations”.

168

169 **Q3:** (3) The calculation of the initial VOC concentrations is problematic: the method
170 depends heavily on initial/source ratio which is not discussed at all in this work; the
171 method assumes biogenic VOCs share the same air mass histories as the anthropogenic
172 VOCs which is not supported by any evidence. For these reasons, I do not recommend
173 the current form of the manuscript for publication in Atmospheric Measurement and
174 Techniques. Given the substantial amount of work needed to demonstrate the
175 robustness of the machine learning workflow, to outline key details in a transparent
176 manner, and to revise the initial VOC calculation, resubmission is recommended. Please
177 see my specific and minor/technical comments below.

178 **Reply:** Thank you so much for your good suggestions. In previous studies (Shao et al.,
179 2011; Zhan et al., 2021), it has been justified for selecting the pair of
180 ethylbenzene/xylene as the tracers when calculating ambient OH exposure in terms of
181 the following rules: 1) the concentrations of xylene and ethylbenzene are well
182 correlated, which indicates that they are simultaneously emitted; 2) they have different
183 degradation rates in the atmosphere; 3) the calculated initial VOCs are in good
184 agreement with those calculated using other tracers, such as toluene/benzene.

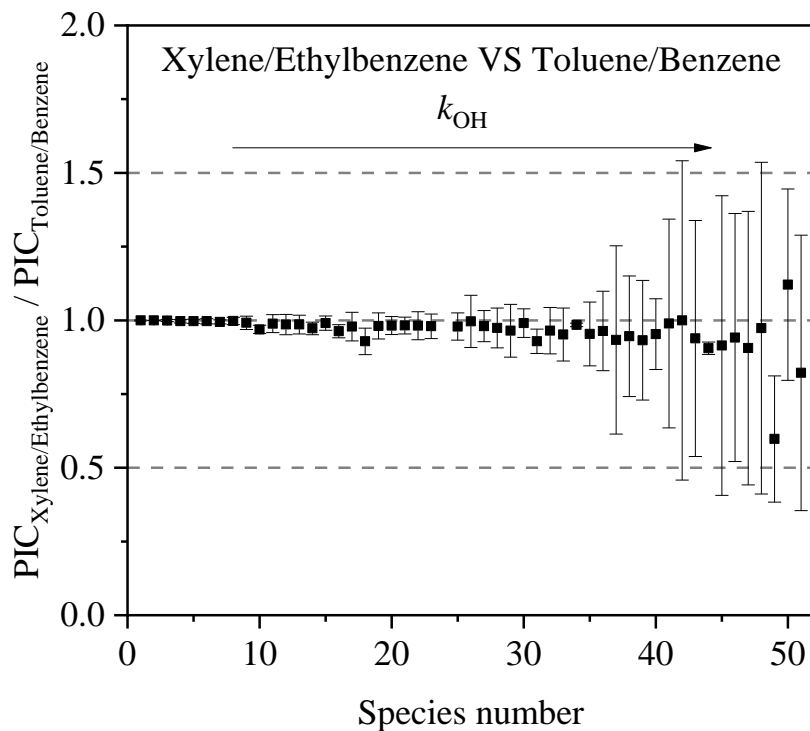
185 As shown in Figure R5 or Figure S9, the concentrations of xylene and
186 ethylbenzene correlated well during our observations in this work. In addition, we
187 compared the ratio of the initial concentrations calculated according to the ratio of
188 xylene/ethylbenzene with that using the ratio of toluene/benzene (Figure R6 or S9).
189 Except for several compounds, the ratio of the PICs for most of these VOCs varied
190 within 1.0 ± 0.1 . This means the calculated photochemical initial concentrations (PICs)
191 are in good agreement when using different tracers. Sensitivity tests showed that the
192 uncertainty caused by the OH exposure (from -10% to $+10\%$) ranged from 0.55 to 1.57
193 (Table R2 or Table S4). Figure R7 or Figure S12 shows the calculated diurnal curves of
194 the PICs from 2014 to 2016. Photochemical losses of VOCs occurred prominently
195 during the daytime.



197

198

Figure R5. The relationship between xylene and ethylbenzene.



199

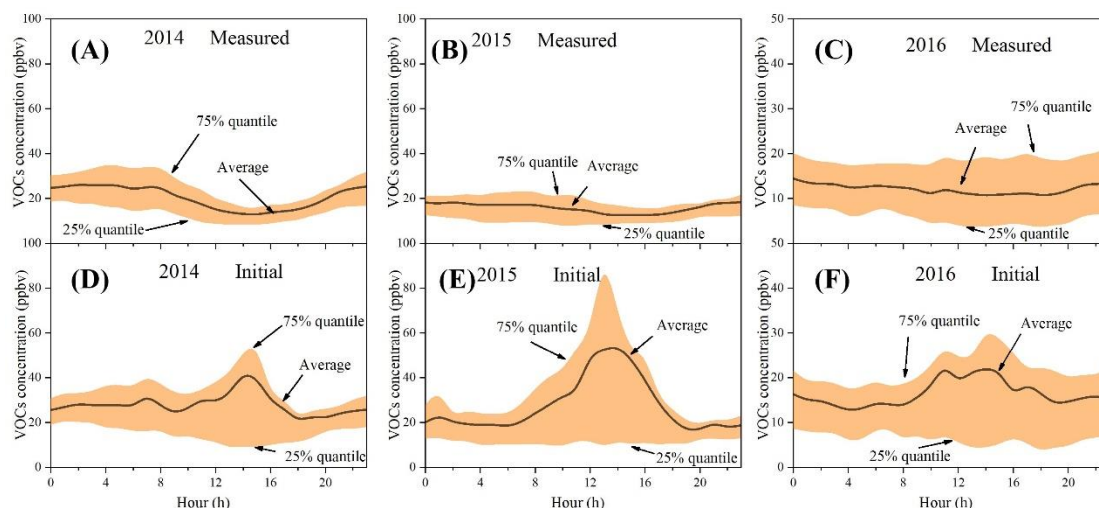
200

201

202

203

Figure R6. Comparison of the initial VOCs calculated using the ratio of xylene/ethylbenzene with that using the ratio of toluene/benzene in 2015. (Error bars are standard deviations.)



204

205 **Figure R7.** The daily variation of VOCs concentration. (A and D for 2014; B and E
 206 for 2015; C and F for 2016)

207

208 **Table R2.** k_{OH} , Method Detection Limit (MDL) and sensitivity test on estimation of
 209 $[OH] \times t$ of different VOC species

Speci	e	species name	k_{OH}^*	MDL**	Ratio to the initial VOC***					
					2014		2015		2016	
numb	er			-10%	+10%	-10%	+10%	-10%	+10%	
				$[OH] \times t$	$[OH] \times t$	$[OH] \times t$	$[OH] \times t$	$[OH] \times t$	$[OH] \times t$	
1		Ethane	0.254	0.050	1.00	1.00	1.00	1.00	1.00	1.00
2		Acetylene	0.756	0.022	1.00	1.00	1.00	1.00	1.00	1.00
3		Propane	1.11	0.013	1.00	1.00	1.00	1.00	1.00	1.00
4		Benzene	1.22	0.011	1.00	1.00	1.00	1.00	1.00	1.00
5		iso-Butane	2.14	0.010	1.00	1.00	1.00	1.00	1.00	1.00
6		2,2-Dimethylbutane	2.27	0.005	1.00	1.00	1.00	1.00	1.00	1.00
7		n-Butane	2.38	0.011	1.00	1.00	1.00	1.00	1.00	1.00
8		2,2,4-Trimethylpentane	3.38	0.008	1.00	1.00	1.00	1.00	1.00	1.00
9		iso-Pentane	3.6	0.008	1.00	1.00	1.00	1.00	1.00	1.00

10	Cyclopentane	5.02	0.005	1.00	1.00	1.00	1.00	1.00	1.00
11	n-hexane	5.25	0.011	0.99	1.01	0.99	1.01	0.99	1.01
12	Toluene	5.58	0.009	1.00	1.00	0.99	1.01	1.00	1.00
13	2,3-Dimethylbutane	5.79	0.004	1.00	1.00	1.00	1.00	0.99	1.01
14	n-Propyl benzene	5.8	0.008	1.00	1.00	1.00	1.00	0.99	1.01
15	iso-Propyl benzene	6.3	0.007	1.01	1.01	0.99	1.01	0.97	1.03
16	2,3,4-trimethylpentane	6.6	0.008	0.99	1.01	0.99	1.01	1.00	1.00
17	n-heptane	6.81	0.009	0.99	1.01	0.99	1.01	0.99	1.01
18	ethylbenzene	7	0.009	0.99	1.01	0.99	1.01	0.99	1.01
19	cyclohexane	7.02	0.011	1.00	1.00	0.99	1.01	0.99	1.01
20	2,3-Dimethylpentane	7.15	0.009	1.00	1.00	1.00	1.00	1.00	1.00
21	3-Methylhexane	7.17	0.009	1.00	1.00	0.99	1.01	1.00	1.00
22	ethene	8.15	0.021	0.99	1.01	0.99	1.01	0.99	1.01
23	n-octane	8.16	0.008	0.99	1.01	1.00	1.00	1.00	1.00
24	2-Methylheptane	8.31	0.008	1.00	1.00	0.99	1.01	0.99	1.01
25	3-Methylheptane	8.59	0.008	1.00	1.00	1.00	1.01	0.99	1.01
26	methylcyclohexane	9.64	0.005	0.99	1.01	0.99	1.01	0.99	1.01
27	n-nonane	9.75	0.006	0.99	1.01	0.99	1.01	0.98	1.02
28	n-decane	11	0.007	0.99	1.01	0.99	1.01	0.99	1.01
29	p-ethyl toluene	11.8	0.007	0.99	1.01	0.98	1.02	0.98	1.02
30	p-diethyl benzene	-	0.008	1.00	1.00	0.99	1.01	0.97	1.03
31	o-ethyl toluene	11.9	0.007	0.99	1.01	0.99	1.01	1.00	1.00
32	o-xylene	13.6	0.007	0.99	1.01	0.98	1.02	1.00	1.00
33	m-ethyl toluene	18.6	0.010	0.99	1.01	0.99	1.01	0.97	1.03
34	m-diethyl benzene	-	0.009	0.99	1.01	0.99	1.01	0.98	1.02
35	m/p-Xylene	23.1/14	0.008	0.99	1.01	0.98	1.02	0.98	1.03

		.2							
36	propene	26	0.015	0.96	1.04	0.95	1.05	0.96	1.05
37	1-Butene	31.1	0.010	0.97	1.04	0.90	1.12	0.92	1.10
38	1-Pentene	31.4	0.009	0.98	1.02	0.93	1.09	0.93	1.08
39	1,2,4-trimethyl benzene	32.5	0.008	1.00	1.01	0.95	1.05	0.91	1.10
40	1,2,3-trimethyl benzene	32.7	0.009	0.96	1.04	0.96	1.04	0.97	1.03
41	a-pinene	51.8	0.010	0.97	1.04	0.96	1.05	0.75	1.35
42	cis-2-Butene	55.8	0.019	0.87	1.16	0.86	1.17	0.77	1.32
43	1,3,5- Trimethylbenzene	56.7	0.007	0.93	1.08	0.90	1.13	0.73	1.37
44	styrene	58	0.010	0.91	1.11	0.90	1.13	0.98	1.02
45	2-methyl-1- pentene	63	0.002	0.81	1.25	0.70	1.49	0.81	1.28
46	trans-2-Butene	63.2	0.014	0.84	1.22	0.82	1.25	0.76	1.35
47	cis-2-Pentene	65	0.006	0.86	1.19	0.74	1.42	0.83	1.24
48	1,3-Butadiene	65.9	0.024	0.88	1.16	0.82	1.26	0.87	1.18
49	trans-2-Pentene	67	0.009	0.88	1.16	0.63	1.63	0.75	1.38
50	β-pinene	73.5	0.010	0.90	1.12	0.81	1.26	0.92	1.10
51	isoprene	99.6	0.009	0.73	1.40	0.67	1.50	0.55	1.57

210 * Unit: $10^{-12} \text{ cm}^3 \text{ mole}^{-1} \text{ s}^{-1}$. k_{OH} values were under conditions of 300K. (Carter 2010)

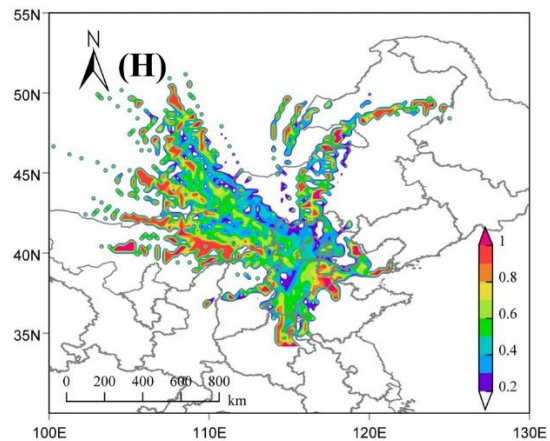
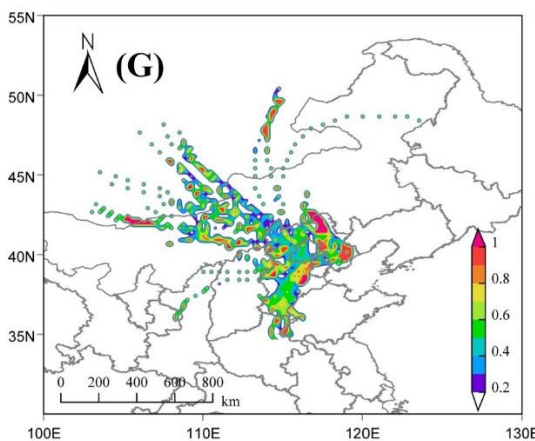
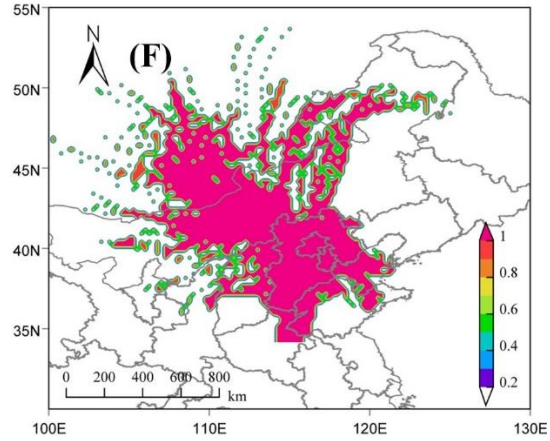
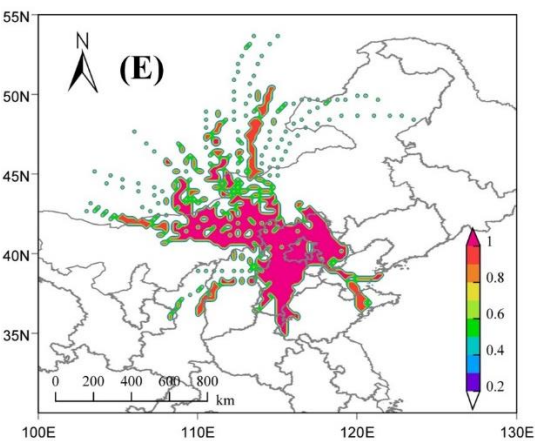
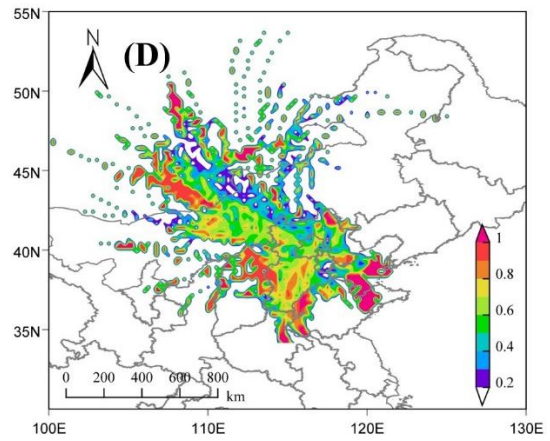
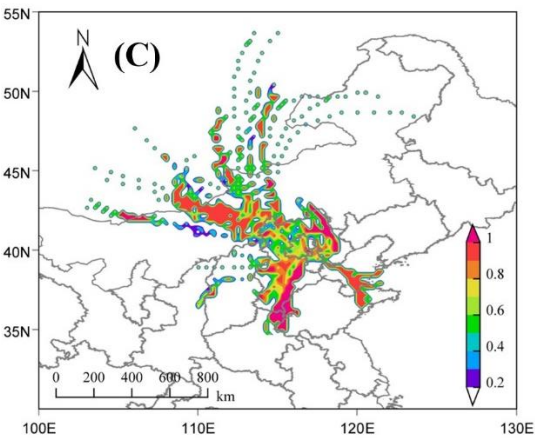
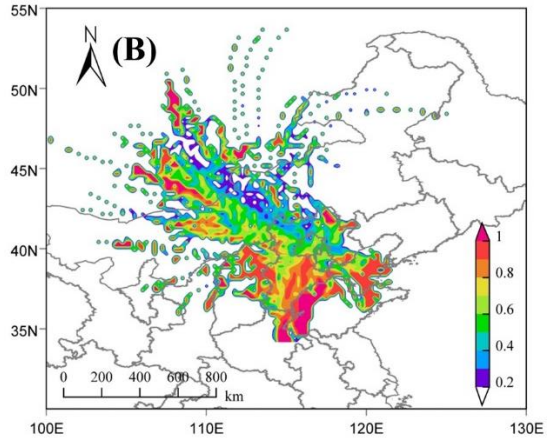
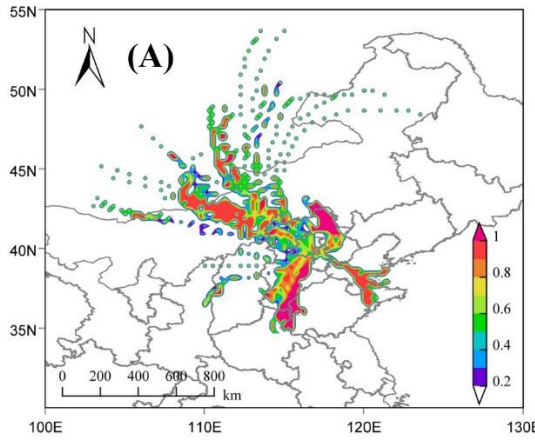
211 ** Unit: ppb. The relative standard derivations (RSDs) were within 10% for the target compounds in all six replicates.

212 *** All species were selected for sensitivity tests of initial VOCs to $[\text{OH}] \times t$. The reaction rates of these species with
 213 OH covered the range of 51 VOCs and were characterized by low, medium and high k_{OH} levels. The sensitivity test
 214 results showed that the uncertainty in the estimation of initial VOCs caused by the $[\text{OH}] \times t$ estimation uncertainty
 215 ranged from 0.55 to 1.57.

216

217 Potential source contribution function (PSCF) analysis has been further carried out
 218 to evaluated the possible influence of air mass on the emission ratio of ethylbenzene

219 and xylene. As shown in Figure R8A-D or Figure S11, xylene showed similar pattern
220 to ethylbenzene in the early morning or in the whole day. These results indicate that
221 variations of air mass should have little influence on their initial ratio. In addition,
222 isoprene showed similar patterns to that of xylene and ethylbenzene (Figure R8G-H),
223 which means VOC emissions are evenly distributed in Beijing. This can be ascribed to
224 the fact that our observation site is a typical urban station. Although isoprene and
225 xylene/ethylbenzene are from biogenic sources and anthropogenic sources, both them
226 are non-point sources on a city scale.



228 Figure R8. The potential source contribution function (PSCF) maps for ethylbenzene
 229 (A and B), xylene (C and D), ratio of xylene to ethylbenzene (E and F), and isoprene
 230 (G and H) arriving in the observation site. The figures A, C, E and G are the results for
 231 the morning (05:00 and 06:00), and the figures of B, D, F and H are the results of the
 232 whole day (00:00-23:00).

233

234 In the revised SI, we added the details on calculation of the initial VOCs and more
 235 discussions in the Text S2. The changes are shown below.

236 **“Text S2. Calculation of initial VOCs concentrations**

237 Photochemical initial concentration (PIC) proposed by Shao et al. (2011), which
 238 is calculated based on the photochemical-age approach and has been applied to evaluate
 239 the effect of photochemical processing on measured VOC levels. Equation S1
 240 essentially describes the integrated OH exposure (Shao et al., 2011).

$$241 \int c_{OH} dt = \frac{1}{k_{A,OH} - k_{B,OH}} \left[\ln\left(\frac{VOC_A}{VOC_B}\right)_{initial} - \ln\left(\frac{VOC_A}{VOC_B}\right) \right] \quad (S1)$$

242 The initial concentration of species i can be calculated using Equation S2.

$$243 VOC_{i, initial} = \frac{VOC_i}{\exp(-k_{i,OH}) \exp(\int c_{OH} dt)} \quad (S2)$$

244 Substituting equation 1 into equation 2, then we can get equation S3.

$$245 VOC_{i, initial} = \frac{VOC_i}{\exp(-k_{i,OH}) \exp\left(\frac{1}{k_{A,OH} - k_{B,OH}} \left[\ln\left(\frac{VOC_A}{VOC_B}\right)_{initial} - \ln\left(\frac{VOC_A}{VOC_B}\right) \right] \right)} \quad (S3)$$

246 Where C_{OH} represents the ambient OH concentration; $k_{A,OH}$ and $k_{B,OH}$ represent the
 247 reaction rate of compound A and B with OH radical, respectively; t represents the
 248 reaction time of species i in the ambient.

249 In previous work (Shao et al., 2011; Zhan et al., 2021), the selection of
 250 ethylbenzene and xylene as tracers was justified for calculating ambient OH exposure
 251 under the following conditions: 1) the concentrations of xylene and ethylbenzene were
 252 well correlated (Figure S9), which indicated that they were simultaneously emitted; 2)
 253 they had different degradation rates in the atmosphere; and 3) the calculated PICs were
 254 in good agreement with those calculated using other tracers (Shao et al., 2011; Zhan et
 255 al., 2021).

256 In this study, the ethylbenzene/xylene pair was used to calculate ambient OH

257 exposure. As shown in Figure S9, the concentrations of xylene and ethylbenzene are
258 well correlated, which indicates that they are simultaneously emitted. In addition, we
259 compared the PICs according to xylene/ethylbenzene with that using toluene/benzene
260 (Figure S10). The calculated PICs ratio ($\text{PIC}_{\text{Xylene/Ethylbenzene}} / \text{PIC}_{\text{Toluene/Benzene}}$) varied
261 from 0.5 to 1.5 with a mean value of 0.96. This means the calculated initial VOCs was
262 in good agreement when using different tracers. The mean ratio (0.52, from 0.45 to 0.66)
263 of ethylbenzene/xylene before sunrise was taken as the initial ratio of
264 ethylbenzene/xylene. Sensitivity tests showed that the uncertainty of PICs caused by
265 the OH exposure (from -10% to +10%) ranged from 0.55 to 1.57 (Table S4).

266 Variations of air mass may also affect the VOC ratio. Figure S11 A-D shows the
267 mean concentration distribution of ethylbenzene and xylene in the early morning and
268 the whole day based on potential source contribution function (PSCF) analysis. Xylene
269 showed similar patterns to ethylbenzene in different air mass trajectories and different
270 periods. These results indicate that the emissions of xylene and ethylbenzene were
271 constant throughout the day and variations of air mass should have little influence on
272 the initial ratio of VOCs. The hourly concentrations of ethylbenzene and xylene were
273 used to calculate the concentration of initial VOCs. The initial VOC was calculated by
274 adding the measured VOC concentration and the calculated photochemical loss. Figure
275 S12 shows the diurnal variations of the observed and initial VOCs concentrations from
276 2014 to 2016. Photochemical loss of VOC occurred mainly during the daytime.

277 It should be noted that the lifetimes ($1/k_{2COH}$) of highly reactive VOCs, such as
278 isoprene, greatly depend on the OH exposure. The photochemical ages of isoprene were
279 0.01–6.21 h (1.26 ± 1.12 h). This value is comparable with previously reported
280 photochemical ages (Shao et al., 2011; Gao et al., 2018). However, the initial
281 concentrations of highly reactive VOCs may be overestimated due to their short
282 lifetimes and should be taken as the upper limits. On the other hand, isoprene is a
283 biogenic VOC, while xylene and ethylbenzene are anthropogenic VOCs. If they do not
284 share the same air mass histories, an additional uncertainty is inevitable for the PICs of
285 isoprene. As shown in Figure S11, isoprene showed similar patterns to that of xylene
286 and ethylbenzene, which means VOC emissions are evenly distributed in Beijing during

287 our observations. This can be ascribed to the fact that our observation site is a typical
288 urban station. Although isoprene and xylene/ethylbenzene different sources, both them
289 are non-point sources on a city scale. Therefore, the photochemical clock calculated
290 using xylene and ethylbenzene is able to correct the photochemical loss of biogenic
291 VOCs to some extent. It should be noted that uncertainty is inevitable when we
292 estimating the photochemical age (Parrish et al., 2007). However, the aim of this work
293 is to test whether the ML-model can reflect the influence of photochemical loss of
294 VOCs species on O₃ modelling. The PICs should provide additional information for
295 understanding O₃ formation in the atmosphere.”.

296 As for the robustness and workflow of RF model, we have replied this point in **Q1**
297 and **Q2** and revised the manuscript and the SI accordingly.

298

299 Specific concerns:

300 **Q4:** Line 70-71: This is a valid concern. However, the machine learning based
301 approaches are also subject to this.

302 **Reply:** Thank you for your comment. We have added a paragraph to point out the
303 shortcoming of machine learn “Although attentions should be paid to the robustness of
304 machine learning because it depends on input dataset (observations or outputs from
305 chemical transport models), previous studies have demonstrated that cross-validation
306 and data-normalization can well reduce the dependence of the model on input data and
307 improve the robustness of the model (Wang et al., 2016; Wang et al., 2017b; Liu et al.,
308 2021; Ma et al., 2021)” in Lines 79-83 in the revised manuscript.

309

310 **Q5:** Line 72-73: Respectfully, I disagree. Box models using condensed mechanisms are
311 usually quite cheap. Near-explicit mechanisms such as MCM are more expensive, but
312 the EKMA-type configurations are still considerably cheaper than 3D chemical
313 transport models. Well-developed box models with MCM or other condensed
314 mechanisms configured for ozone sensitivity (EKMA) can run on personal computers
315 or small servers/clusters, providing timely predictions with no major demand for
316 computational resources. OBMs generally are not considered as being time-consuming

317 or computationally expensive.

318 **Reply:** Thank you. We have deleted the sentences “In addition, both of them are time-
319 consuming and expensive when computational resources are considered” and
320 “Traditional models have difficulty assessing O₃ formation sensitivity in a timely
321 manner due to the limitations of flexibility and computational efficiency” in the revised
322 manuscript.

323

324 **Q6:** Line 79-90: This section lists a few previous studies with vaguely portrayed
325 methodologies and outcomes, but failed to mention any disadvantages of machine
326 learning, such as the demand for large volume of comprehensive and good quality data,
327 and of course the risk of overtraining. This section also fails to address a concern
328 brought up earlier by the authors themselves: uncertainties and biases in the input
329 dataset (observations, or outputs from chemical transport models). Please revise this
330 section and discuss the applications of machine learning in air quality studies in the
331 context of its disadvantages. Please also address how the impacts of input data (e.g.,
332 uncertainties and biases) might be reduced.

333 **Reply:** Thank you. We have revised this section and added the discussion in lines 79-
334 86 in the reversed manuscript “**Although attentions should be paid to the robustness of**
335 **machine learning because it depends on input dataset (observations or outputs from**
336 **chemical transport models), previous studies have demonstrated that cross-validation**
337 **and data-normalization can well reduce the dependence of the model on input data and**
338 **improve the robustness of the model (Wang et al., 2016; Wang et al., 2017b; Liu et al.,**
339 **2021; Ma et al., 2021). Thus, it is a promising alternative to account for the effects of**
340 **meteorology on air pollutants and has been intensively used in atmospheric study (Liu**
341 **et al., 2020; Hou et al., 2022).”.**

342

343 **Q7:** Line 135-137: “... and then averages the scores of each decision tree as its final
344 score...” This is a very vague description of the algorithm. Indeed, the ensemble
345 prediction made by the entire forest is usually more accurate and robust than the
346 predictions made by individual trees, relatively speaking. However, this (averaging

347 across all the decision trees) ABSOLUTELY DOES NOT guarantee that large biases
348 and overfitting can be avoided. The splitting might help with mitigating the risk of
349 overfitting but it is still FAR FROM BEING SUFFICIENT to guarantee the algorithm
350 is not overfitted. Generally, much more comprehensive and rigorous measures than
351 what is shown in this work are needed, for instance, multifold cross validation is a good
352 idea. To further test the robustness of the machine learning workflow in real-world
353 physics-driven problems, sometimes it is recommended to perform the cross validation
354 with each fold being the data from a specific time period or geographic region.

355 **Reply:** Thank you so much for your good suggestion. We agree with you that the
356 splitting might help with mitigating the risk of overfitting but it is still not sufficient to
357 guarantee the algorithm is not overfitted. As replied in above questions, we performed
358 multifold cross-validation according to your suggestion. A 12-fold cross-validation was
359 carried out to mitigate the risk of overfitting. Briefly, we randomly divided the
360 normalized data into 12 subsets, then alternately took one subset as testing data along
361 with the rest as training data. By doing this, every data point has an equal chance being
362 trained and tested.

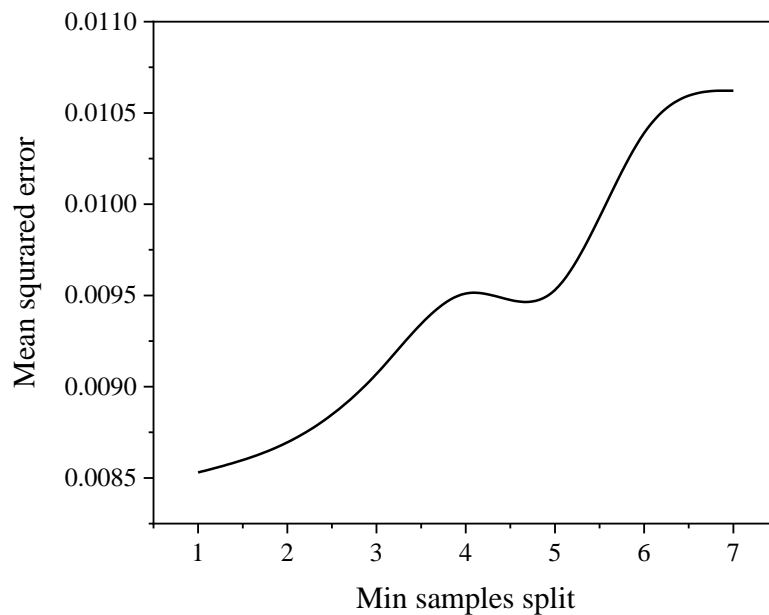
363 In lines 145-153 in the revised manuscript, we have revised the sentence "... and
364 then averages the scores of each decision tree as its final score..." to "**The random forest
365 (RF) is a type of ensemble decision tree that can be used for classification and
366 regression (Breiman 2001).** During the training process, the model creates a large
367 number of different decision trees with different sample sets at each node, and then
368 averages the results of all decision trees as its final results (Breiman 2001). **To avoid
369 over-fitting, we trained the random forest model using cross-validation for the
370 normalized data, which can improve the robustness of the model. Briefly, we randomly
371 divided the normalized data into 12 subsets, then alternately took one subset as testing
372 data along with the rest as training data. By doing this, every data point has an equal
373 chance being trained and tested.**".

374

375 **Q8:** Line 132-: this section does not provide any details on whether the authors have
376 performed any sort of hyperparameter tuning, which is important. How can the readers

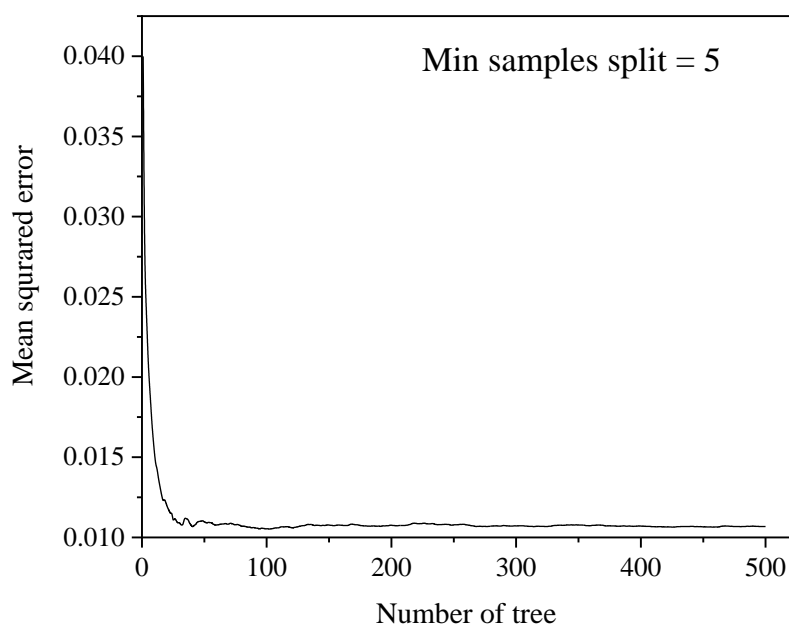
377 be convinced that the performance is optimized? Information outlined in Table S1 is
378 not at all sufficient to described how the algorithm is configured. And frankly, certain
379 information in that table is practically useless (e.g., the method is "regression", and the
380 sampling is "random"). Please also clarify if the authors implemented random forest by
381 themselves or used that from a certain package (e.g., R, python). If latter, please specify
382 which package is used.

383 **Reply:** Thank you for you good comments. In the revised SI, we added the process of
384 hyperparameter tuning, such as the influence of the min sample split (Figure R9 or
385 Figure S13) and tree number (Figure R10 or Figure S14) on the mean squared error
386 (MSE). We also revised Table S2 (Table R3). We implemented random forest
387 simulation by ourselves. The code was written by ourselves based on a MATLAB
388 platform.



389

390 **Figure R9.** The relationship between min sample split and mean squared error (MSE)



391

392 **Figure R10.** The relationship between trees number and mean squared error (MSE).

393

394

Table R3. RF model parameters and input parameters

RF model parameters		RF model inputs		
Type	Value	Type	input parameter	output parameter
Cross-validation	12	Figure 2A	Total VOC concentration, PM _{2.5} , NO, NO ₂ , CO, SR, RH, WD, WS, T	O ₃
tree number	500	Figure 2B	51 measured VOC species, PM _{2.5} , NO, NO ₂ , CO, SR, RH, WD, WS, T	O ₃
min sample split	5	Figure 2C	51 initial VOC species, PM _{2.5} , NO, NO ₂ , CO, SR, RH, WD, WS, T	O ₃
min sample leaf	1			

395 Note: In this study, we optimized the number of tree and min samples split as shown

396 in Figure S14 and S13, respectively. The min sample leaf was set 1 (default), and

397 other parameter were set to default (auto/none).

398 Min samples split: the minimum number of samples to be split; Min samples leaf: the
399 minimum number of samples in a leaf; Trees number: the number of trees during the
400 training.

401

402 In lines 166-168 in the revised manuscript, we added a sentence “More details
403 about workflow of RF model and the hyperparameter tuning can be found in the Text
404 S3. The optimized parameters are shown in Table S2”.

405 In the revised SI, we added a short paragraph to describe the process of
406 hyperparameter tuning “(3) Hyper-parameters optimization. All network configuration
407 parameters (i.e., leaf number, number of trees, algorithm, and so on) were modified by
408 a trial and error method to obtain the optimized network structure. The optimized RF
409 model parameters are shown in Table S2. Figures S12 and S13 show the examples to
410 optimize the number of min sample split and tree, respectively.”.

411

412 **Q9:** Line 143, 145: please clarify how this “tiny data noise” is added.

413 **Reply:** Thank you. The “tiny data noise” was through randomly permutes the
414 observations of feature i . We have revised it to “errOOB1 and errOOB2 represent the
415 out-of-bag data error of feature i before and after randomly permuting the observation,
416 respectively.” in line 163-165 in the revised manuscript.

417

418 **Q10:** Line 147-150: I am not sure what the purpose is. Given the atmospheric lifetime
419 of ozone, the measurements may well carry some “memory effects”. Do the authors
420 suggest that the ozone records can be reconstructed with randomly arranged inputs and
421 hence any transport footprint (and factors alike) is already captured by the suite of
422 instantaneous measurements?

423 **Reply:** Thank you. we agree with you that the measurements (especially O₃) may carry
424 some “memory effects”. However, it is inevitable that some “memory effects” cannot
425 be considered. In order to decrease the dependence of the model on the data, we fed the
426 randomly arranged inputs to the model by interrupting the continuity of the time series
427 to check the robustness of the model. It is actually a cross-validation but with a smaller

428 fold (not systematic) than that used in the revised manuscript, in which we carried out
429 a 12-fold cross-validation to split the training and testing data according to your
430 suggestion. Therefore, the results are more robust in the revised manuscript. We deleted
431 the sentence “we interrupted the continuity of the time series, fed the randomly arranged
432 inputs to the model” in the revised manuscript, and added the detailed workflow in the
433 Text S3.

434

435 **Q11:** Line 160: It is unclear how the initial VOC concentrations are derived. I do notice
436 that Text S2 in the supplement information is about initial VOCs. Please refer to SI
437 contents whenever necessary. I also have several major concerns regarding the initial
438 VOC calculations in Text S2: (1) these formulations require initial/source ratios. It
439 remains absolutely unclear how the authors derive the initial or source ratio of
440 ethylbenzene/xylene. (2) The initial/source ratios may vary among different sources
441 (e.g., gasoline, diesel, combustion, ...). How would the authors account for the impacts
442 from different emission sources? Or the mix with air masses with different
443 photochemical ages? (3) Ethylbenzene and xylene are primarily of anthropogenic origin.
444 The underlying assumption here is that all VOCs experience similar transport and aging
445 processes. This may not be a bad assumption for other anthropogenic VOCs, but I doubt
446 this could be applied for biogenic VOCs, which, according to the authors (Line 261 and
447 Figure 3), is quite important. To sum up, I am not convinced that the initial VOC
448 calculation presented in this manuscript can accurately describe the VOC oxidation
449 during the transport receptor site.

450 **Reply:** Thanks for your comments. In the revised manuscript, we referred to SI contents
451 accordingly, such as, “**The calculation of initial VOCs and sensitivity tests can be found**
452 **in the Supplemental Materials (S2)**” in lines 142-143 and 190-191.

453 We took the mean value (0.52) of ethylbenzene/xylene from 0.45 to 0.66 before
454 sunrise during our observations as the initial ratio of ethylbenzene/xylene. The protocol
455 is the same as that reported in literatures (Shao et al., 2011; Zhan et al., 2021).

456 We agree with you that the initial/source ratios may vary among different sources
457 (e.g., gasoline, diesel, combustion). Here, we used the ambient concentrations of

458 ethylbenzene and xylene to calculate the initial source ratio. Thus, it actually reflects a
 459 mean or mixing value of different sources instead of a specific one. There is a basic
 460 assumption that emission patterns of different sources are relatively stable in a day
 461 when calculating the photochemical initial concentrations of VOCs using this method
 462 (Yuan et al., 2013). As replied in the third question (Q3), we checked this assumption
 463 based on PSCF analysis. The results suggest that the emission patterns of xylene and
 464 ethylbenzene are highly similar in the early morning to that in the whole day.

465 Although xylene and ethylbenzene are anthropogenic VOCs, while isoprene is a
 466 biogenic VOC, PSCF analysis indicated that the spatial pattern of isoprene was similar
 467 to that of xylene and ethylbenzene during our observations (Figure R8). This means
 468 VOC emissions were evenly distributed in Beijing. This can be ascribed to the fact that
 469 our observation site is a typical urban station and VOCs are emitted from non-point
 470 sources on a city scale. Therefore, the photochemical clock calculated using xylene and
 471 ethylbenzene is able to correct the photochemical loss of biogenic VOCs to some extent.

472 In Text S2 in the revised SI, we added more details to calculate the initial
 473 concentrations of VOCs.

474 **“Text S2. Calculation of initial VOCs concentrations**

475 **Photochemical initial concentration (PIC) proposed by Shao et al. (2011), which**
 476 **is calculated based on the photochemical-age approach and has been applied to evaluate**
 477 **the effect of photochemical processing on measured VOC levels. Equation S1**
 478 **essentially describes the integrated OH exposure (Shao et al., 2011).**

$$479 \int c_{OH} dt = \frac{1}{k_{A,OH} - k_{B,OH}} \left[\ln\left(\frac{VOC_A}{VOC_B}\right)_{initial} - \ln\left(\frac{VOC_A}{VOC_B}\right) \right] \quad (S1)$$

480 The initial concentration of species *i* can be calculated using Equation S2.

$$481 VOC_{i, initial} = \frac{VOC_i}{\exp(-k_{i,OH}) \exp(\int c_{OH} dt)} \quad (S2)$$

482 Substituting equation 1 into equation 2, then we can get equation S3.

$$483 VOC_{i, initial} = \frac{VOC_i}{\exp(-k_{i,OH}) \exp\left(\frac{1}{k_{A,OH} - k_{B,OH}} \left[\ln\left(\frac{VOC_A}{VOC_B}\right)_{initial} - \ln\left(\frac{VOC_A}{VOC_B}\right) \right] \right)} \quad (S3)$$

484 **Where C_{OH} represents the ambient OH concentration; $k_{A,OH}$ and $k_{B,OH}$ represent the**
 485 **reaction rate of compound A and B with OH radical, respectively; t represents the**
 486 **reaction time of species *i* in the ambient.**

487 In previous work (Shao et al., 2011; Zhan et al., 2021), the selection of
488 ethylbenzene and xylene as tracers was justified for calculating ambient OH exposure
489 under the following conditions: 1) the concentrations of xylene and ethylbenzene were
490 well correlated (Figure S9), which indicated that they were simultaneously emitted; 2)
491 they had different degradation rates in the atmosphere; and 3) the calculated PICs were
492 in good agreement with those calculated using other tracers (Shao et al., 2011; Zhan et
493 al., 2021).

494 In this study, the ethylbenzene/xylene pair was used to calculate ambient OH
495 exposure. As shown in Figure S9, the concentrations of xylene and ethylbenzene are
496 well correlated, which indicates that they are simultaneously emitted. In addition, we
497 compared the PICs according to xylene/ethylbenzene with that using toluene/benzene
498 (Figure S10). The calculated PICs ratio ($\text{PIC}_{\text{Xylene/Ethylbenzene}} / \text{PIC}_{\text{Toluene/Benzene}}$) varied
499 from 0.5 to 1.5 with a mean value of 0.96. This means the calculated initial VOCs was
500 in good agreement when using different tracers. The mean ratio (0.52, from 0.45 to 0.66)
501 of ethylbenzene/xylene before sunrise was taken as the initial ratio of
502 ethylbenzene/xylene. Sensitivity tests showed that the uncertainty of PICs caused by
503 the OH exposure (from -10% to +10%) ranged from 0.55 to 1.57 (Table S4).

504 Variations of air mass may also affect the VOC ratio. Figure S11 A-D shows the
505 mean concentration distribution of ethylbenzene and xylene in the early morning and
506 the whole day based on potential source contribution function (PSCF) analysis. Xylene
507 showed similar patterns to ethylbenzene in different air mass trajectories and different
508 periods. These results indicate that the emissions of xylene and ethylbenzene were
509 constant throughout the day and variations of air mass should have little influence on
510 the initial ratio of VOCs. The hourly concentrations of ethylbenzene and xylene were
511 used to calculate the concentration of initial VOCs. The initial VOC was calculated by
512 adding the measured VOC concentration and the calculated photochemical loss. Figure
513 S12 shows the diurnal variations of the observed and initial VOCs concentrations from
514 2014 to 2016. Photochemical loss of VOC occurred mainly during the daytime.

515 It should be noted that the lifetimes ($1/k_{2\text{COH}}$) of highly reactive VOCs, such as
516 isoprene, greatly depend on the OH exposure. The photochemical ages of isoprene were

517 0.01–6.21 h (1.26 ± 1.12 h). This value is comparable with previously reported
518 photochemical ages (Shao et al., 2011; Gao et al., 2018). However, the initial
519 concentrations of highly reactive VOCs may be overestimated due to their short
520 lifetimes and should be taken as the upper limits. On the other hand, isoprene is a
521 biogenic VOC, while xylene and ethylbenzene are anthropogenic VOCs. If they do not
522 share the same air mass histories, an additional uncertainty is inevitable for the PICs of
523 isoprene. As shown in Figure S11, isoprene showed similar patterns to that of xylene
524 and ethylbenzene, which means VOC emissions are evenly distributed in Beijing during
525 our observations. This can be ascribed to the fact that our observation site is a typical
526 urban station. Although isoprene and xylene/ethylbenzene different sources, both them
527 are non-point sources on a city scale. Therefore, the photochemical clock calculated
528 using xylene and ethylbenzene is able to correct the photochemical loss of biogenic
529 VOCs to some extent. It should be noted that uncertainty is inevitable when we
530 estimating the photochemical age (Parrish et al., 2007). However, the aim of this work
531 is to test whether the ML-model can reflect the influence of photochemical loss of
532 VOCs species on O₃ modelling. The PICs should provide additional information for
533 understanding O₃ formation in the atmosphere.”.

534

535 **Q12:** Line 176-177: Simply comparing RF outputs to measurements ABSOLUTELY
536 DOES NOT guarantee that the RF model is robust. An over-trained model will also
537 show good performance when evaluated with measurements. Figure 2 says nothing
538 about the robustness of the model.

539 **Reply:** Thank you so much. We agree with you that simply comparing RF outputs to
540 measurements absolutely does not guarantee that the RF model is robust. We have
541 carried out cross-validation in the revised manuscript according to your good
542 suggestion. The details on the robustness of the model have been replied in Q1 and Q2.
543 All the figures (Figure 2, Figure S3 and Figure S4) have been updated in the revised
544 manuscript and the revised SI.

545

546 **Q13:** Line 221-222: The authors stated that “ML is a black-box model” then cited

547 Sayeed et al. (2021). Do the authors then imply that the convolutional neural network
548 model developed by and described in Sayeed et al is a “black-box”? If this is the case,
549 please elaborate how the Sayeed et al model appears to be a black-box to the authors,
550 since this is a somewhat strong accusation. I also do not fully agree with this statement.
551 Random forest is actually fairly transparent compared to some other types of machine
552 learning algorithms, as one can certainly examine the trees and see how a certain feature
553 is used for splitting the nodes and how the overall importance is propagated, if they
554 wish.

555 **Reply:** Thank you. We agree with you that when compared with other types of machine
556 learning algorithms, random forest is actually fairly transparent because one can
557 examine every node. However, when compared with chemical models, such as box
558 model and chemical transport model. It is still a “black box” from the point view of
559 chemical mechanism. In lines 116-118 in the revised manuscript, we revised this
560 sentence to “Although ML is widely used to understand air pollution, explanations of
561 ML results (e.g., RI) are somewhat vague because ML is a black-box model **from the**
562 **point view of chemical mechanism**”.

563

564 **Q14:** Line 267-270, Line 287-293: Please clarify how the EKMA plots were generated
565 using the RF model. It is confusing that Figures 4A-C and Figure 4D use different color
566 scales. It also appears to me that Figure 4B and Figure 4D show considerable
567 discrepancy: the “observed point” in Figure 4B indicates ~44 ppb ozone but in Figure
568 4D the ozone level at the “observed point” is ~60 ppb. Please also define this “observed
569 point”. It could be that the OBM predicts some sort of “maximum ozone production
570 potential” driven by chemistry and impacts like transport would not be captured. But
571 this would be inconsistent with one of the conclusions of this work (e.g., Line 206) that
572 ozone production seems to be dominated by local chemistry. Either way, the
573 discrepancy needs to be elaborated.

574 **Reply:** Thank you for your good comment. In the revised SI, we have added the
575 calculation process of EKMA in Text S3. This has also been replied in **Q2**. In lines 171-
576 179 in the revised manuscript, we added a paragraph “**When plotting the O₃ formation**

577 sensitivity curves, we made a virtual matrix of inputs by varying the concentrations of
578 NO_x and VOCs from 0.9 to 1.1 times (with a step of 0.01) of their mean values while
579 keeping all other inputs unchanged (i.e., the mean values). Then, the new matrix was
580 used as testing data, while all the measured data were taken as training data. Thus, the
581 testing data should represent the mean sensitivity regime of O₃ in Beijing, while the
582 training data actually covered all the sensitivity regimes of O₃ formation. The EKMA
583 curves were plotted using the daily maximum 8-h (MDA8) O₃. More details can be
584 found in the SI”.

585 In the initial submission version of the manuscript, the EKMA curves based on the
586 RF model were plotted using the mean O₃ concentrations in a day with different color
587 scale, while the EKMA curves from the Box model were plotted using the maximum
588 O₃ concentrations in a day. This leads to the difference in O₃ concentrations between
589 Figure 4B and 4D. In the revised manuscript, we plotted the EKMA curves from both
590 models using the daily maximum 8-h (MDA8) O₃ with the same scale. As shown in
591 Figure R3 or Figure 4. The predicted O₃ concentrations using two different models are
592 comparable. In addition, we calculated the relative errors (within 15.6%) of O₃
593 concentrations from the RF model compared with that of the Box model (Figure R4 or
594 Figure S8). The observed point has been added in the revised Figure 4 or Figure R3.

595 In Text S3 in the revised SI, we have added the details for plotting EKMA curves: “(6)
596 EKMA curves. The Empirical Kinetic Modeling Approach (EKMA) was used to assess
597 the O₃ formation mechanism regime. Both the RF model and a box model with Master
598 Chemical Mechanism (MCM, 3.3.1) were used to calculate the EKMA curves. For the
599 RF model simulations, the observed point data was chosen as the mean values of the
600 input parameters during our observations, then the concentrations of VOCs and NO_x
601 were varied $\pm 10\%$ (or from 90% to 110%) of their mean values with a step of 1% in a
602 two-dimensional matrix along with other inputs unchanged. This matrix was used as
603 the testing data, while all the measured data were taken as the training data in the RF
604 model to simulate O₃ concentrations under different scenarios of VOCs and NO_x
605 concentrations. To decrease the model uncertainty, we set relatively small variations of
606 VOCs and NO_x ($\pm 10\%$) compared to the observed values in this study. The mean

607 relative error of simulated O₃ concentrations between RF model and Box model (within
608 15.6%, Figure S8) suggests that the RF model can well predict O₃ concentrations during
609 our observations.”.

610

611 **Q15:** Line 299-301: I actually fail to see this. Figures 2E and 2F show that the
612 improvement is small.

613 **Reply:** Thank you. In the revised manuscript, we have revised the sentence “Thus, our
614 model has good prediction performance ($R^2 = 0.87$) when combined with the initial
615 VOC species...and identify the connection between the reactivity of VOC species and
616 O₃ formation in the atmosphere” to “When the TVOCs were split into measured or
617 initial VOC species, the R^2 increased obviously as the number of data features increased.
618 Therefore, the VOC composition has a significant influence on O₃ prediction using the
619 RF model.” in Lines 221-223 in the revised manuscript. Meanwhile, we added “To
620 verify the stability of the model, we performed a significance test on the model results.
621 The results showed that there was no significant difference among the different tests
622 ($P>0.05$, $R^2>0.98$).” in Lines 168-170 in the revised manuscript.

623

624 Minor/technical comments:

625 **Q16:** Line 16: Beijing, China.

626 **Reply:** Thank you. It has been corrected in Line 14 in the revised manuscript.

627

628 **Q17:** Line 21: Define abbreviations upon first appearance. NO_x and PM_{2.5} are not
629 defined. Also, x should be subscripted throughout.

630 **Reply:** Thank you. We have defined the abbreviations when it first appears, such as
631 “nitrogen oxides (NO_x) and relative humidity (RH), and a positive response to
632 temperature (T), solar radiation (SR)” and “fine particulate matter with aerodynamic
633 diameter less than 2.5 μm (PM_{2.5})” in Lines 22 and 95-96. The “x” in NO_x has been
634 subscripted throughout the paper.

635

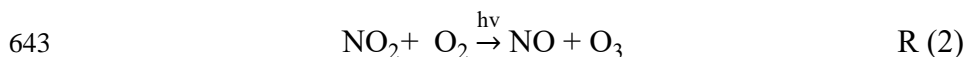
636 **Q18:** Line 22: Delete curves

637 **Reply:** Thank you. We have deleted the “curves”

638

639 **Q19:** Line 33: “NO-O₃-NO₂ cycle” please elaborate. The audience will appreciate
640 clearly described concepts.

641 **Reply:** Thank you. The “NO-O₃-NO₂ cycle” can be expressed by eq. R (1) and R (2).



644 We have revised “NO-O₃-NO₂ cycle” to “**conversion from NO to NO₂, subsequently,**
645 **formation of O₃ by photolysis of NO₂ in the presence of O₂”** in Line 36 in the revised
646 manuscript.

647

648 **Q20:** Line 31-34: Very busy and ill-formed sentence. Please rephrase.

649 **Reply:** Thank you. We have revised this sentence to “**Oxidation of volatile organic**
650 **compounds (VOCs) will produce peroxy radicals (RO₂) and hydroperoxy radicals**
651 **(HO₂). The RO₂/HO₂ can accelerate conversion from NO to NO₂, subsequently,**
652 **formation of O₃ by photolysis of NO₂ in the presence of O₂ (Wang et al., 2017a)**” in
653 lines 34-37 in the revised manuscript.

654

655 **Q21:** Line 52-53: “In addition, this method lacks the predictability of O₃ concentrations
656 for policy-making.” This is a bizarre statement. By definition, observations do not have
657 predictability.

658 **Reply:** Thank you. We have deleted this statement in the revised manuscript.

659 **Q22:** Line 53: OBM can use remote sensing measurements too.

660 **Reply:** Thank you. We have revised to “OBMs combine *in-situ* field observations,
661 remote sensing measurements and chemical box models, which...” in Line 56 in the
662 revised manuscript.

663

664 **Q23:** Line 80: has -> have.

665 **Reply:** Thank you. We have revised “has” to “have” in Line 88 in the revised

666 manuscript.

667

668 **Q24:** Line 99: please fix citation style as per the journal requirements.

669 **Reply:** Thank you. We have fixed citation style as per the journal requirements in the
670 revised manuscript.

671

672 **Q25:** Line 98-100: “Makar et al (1999) reported that highly reactive species, such as
673 isoprene, were underestimated by 40% when the OH reactions were ignored” This is
674 confusing as currently written, which is also a misinterpretation of the paper. Makar et
675 al. clearly stated that it is the isoprene emissions that are underestimated if the OH
676 oxidation is not considered.

677 **Reply:** Thank you. We have revised it to “the isoprene emissions were underestimated
678 by up to 40% if the OH oxidation is not considered.” in Lines 109-110 in the revised
679 manuscript.

680

681 **Q26:** Line 101: Please clearly define what exactly “initial concentration” is. It is my
682 opinion that this concept is vague: if one attempts to measure this “initial concentration”,
683 how close shall the sensor be placed? When it comes to biogenic compounds like
684 isoprene, shall the sensor be placed at the leaf level, within the canopy, or what?

685 **Reply:** Thank you. The “initial concentration” is a concept based on reaction time
686 instead of location or space. It is defined as the concentrations of VOCs before
687 degradation has occurred in a day and actually extrapolated according to a “chemical
688 clock” (OH exposure).

689 In lines 118-121 in the revised manuscript, we clarified it “In this study, we used
690 the RF model to evaluate the prediction performance of atmospheric O₃ using the
691 TVOCs, measured VOC species and photochemical initial concentration (PIC) of VOC
692 species, which is calculated based on the photochemical-age approach (Shao et al.,
693 2011)” and in the revised SI, we added a sentence “Photochemical initial concentration
694 (PIC) proposed by Shao et al. (2011), which is calculated based on the photochemical-
695 age approach and has been applied to evaluate the effect of photochemical processing

696 on measured VOC levels”.

697

698 **Q27:** Line 133: Random forest is not a type of decision tree. It is a collection of a
699 number of decision trees.

700 **Reply:** Thank you. We have revised it to “The random forest (RF) is a type of ensemble
701 decision tree that can be used for classification and regression” in Line 145 in the
702 revised manuscript.

703

704 **Q28:** Line 132-: this section does not mention anything about how these input variables
705 are pre-processed: are extreme values removed? Do the authors apply any
706 standardization or normalization? These variables are on very different numerical scales
707 and sometimes standardization could improve the stability and/or performance.

708 **Reply:** Thank you. We carried out data-normalization and removed the extreme values
709 before modelling. In the revised SI, we clarified it and added the data processing in Text
710 S3 “(2) Data process. After the extreme values were removed, all data were normalized
711 (between 0 and 1) in order to decrease the sample distribution range, accelerate
712 calculation efficiency and improve the robustness of the RF model. Then, the dataset
713 was randomly divided into 12 subsets. Thus, a 12-fold cross-validation was performed
714 by alternately taking one subset as testing data and the rest as training data to ensure
715 that each data point has an equal chance being trained and tested.”.

716

717 **Q29:** Line 136: Please define “score”.

718 **Reply:** Thank you. To describe the random forest more accurately, we have revised
719 “score” to “result” in line 146-148 in the revised manuscript.

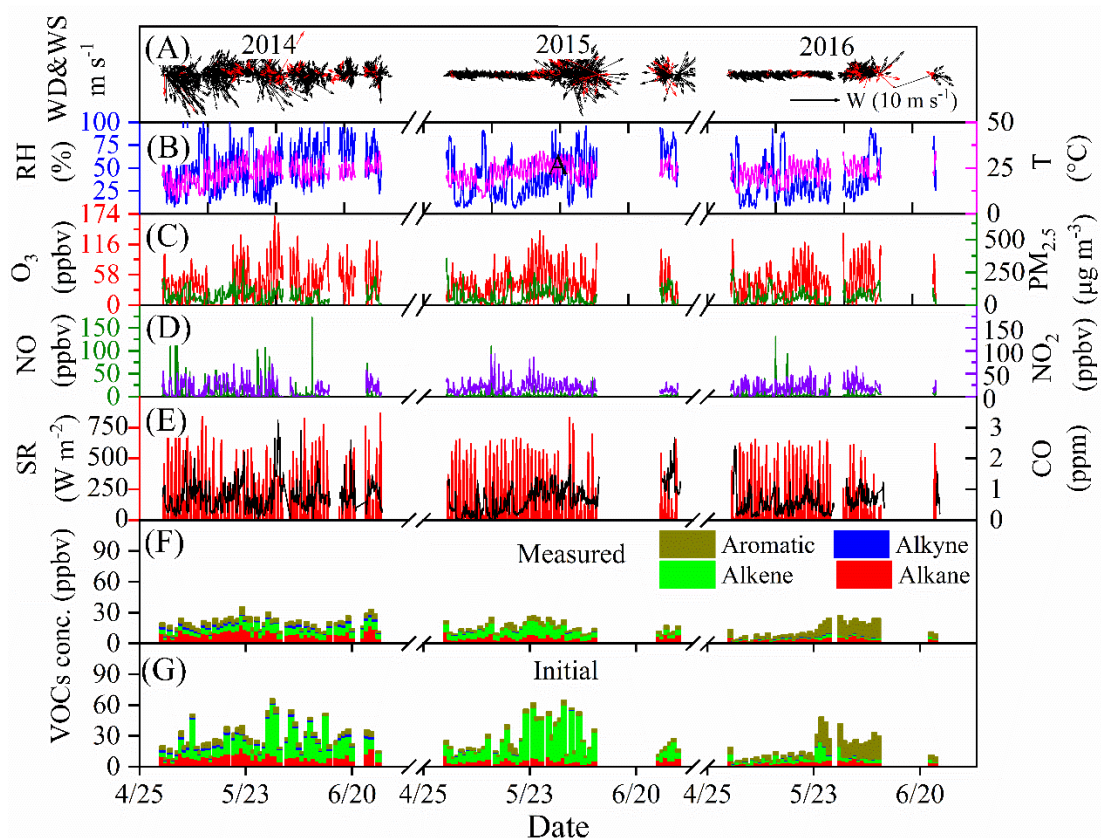
720 “During the training process, the model creates a large number of different decision
721 trees with different sample sets at each node, and then averages the results of all
722 decision trees as its final results”.

723

724 **Q30:** Figure 1: what are those red arrows in the top panel?

725 **Reply:** Thank you. The red arrows represent the O₃ concentration exceeding 74.6 ppbv

726 according to the national ambient air quality standard. We have added this explanation
 727 in Figure 1 or Figure R11 in Lines 205-206 in the revised manuscript.



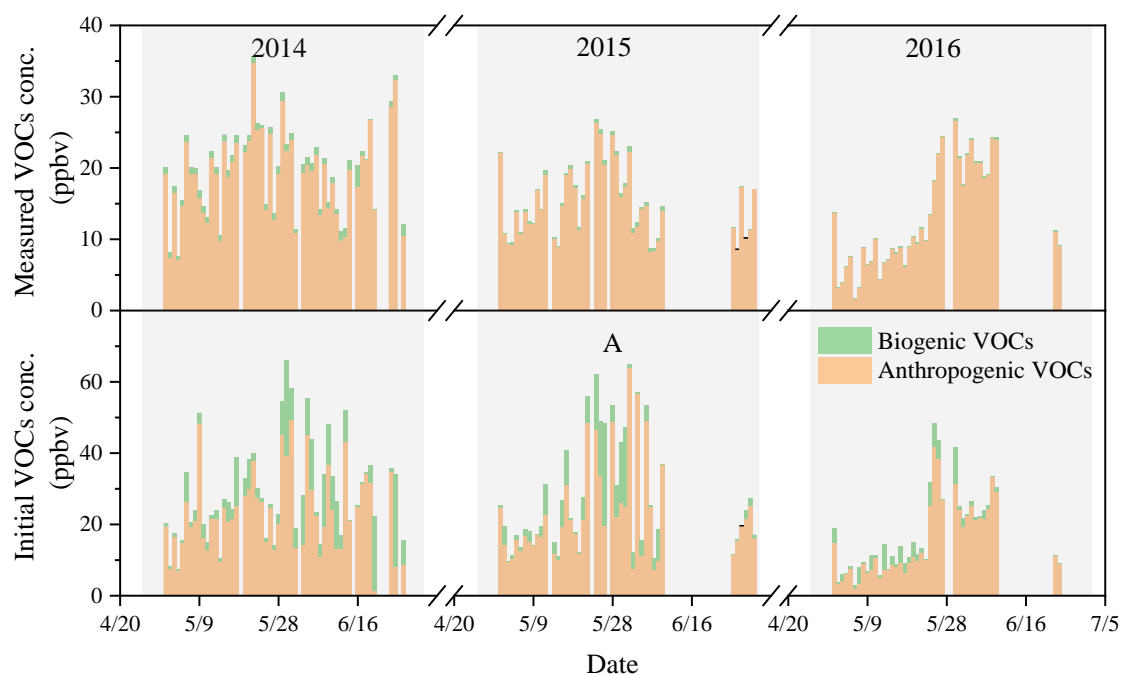
728

729 **Figure R11.** Time series of air pollutants and meteorological parameters during
 730 observations in Beijing. (In A, the red arrows represent the O₃ concentration exceed
 731 74.6 ppbv according to the national ambient air quality standard.)

732

733 **Q31:** Figure 1: it would be interesting to separate biogenic VOCs from anthropogenic
 734 VOCs.

735 **Reply:** Thank you. In this figure, we want to show the general characteristics of
 736 different kinds of VOCs. It is usually classified according to the structures of VOCs.
 737 Figure R12 shows the time series of biogenic and anthropogenic VOCs. We also added
 738 this figure in the revised SI (Figure S16).



739

740 **Figure R12.** Time series of biogenic and anthropogenic VOCs during the observation
 741 period. (Biogenic VOCs: including isoprene, α -pinene and β -pinene; Anthropogenic
 742 VOCs: including all detected VOCs except isoprene, α -pinene and β -pinene)

743

744 **Q32:** Figure 2: all top panels are not readable. Please consider extending the time series
 745 plots.

746 **Reply:** Thank you. We have revised Figure 2 (or Figure R2) in the revised manuscript.

747

748 **Q33:** Text S1: "total of 51 VOCs (including 21 alkanes, 13 alkenes, 1 alkyne and 16
 749 aromatics) were analyzed within a limit of quantification of 0.1-100 ppbv". Well this is
 750 a very wide range for limit of quantification. Please include a table and list the limits of
 751 quantification/detection for all VOCs used in this work. I'd argue that if the LOQ/LOD
 752 of an ambient VOC is on the order of 100 ppb, the data is practically useless. The total
 753 VOC levels are less than ~ 30 ppb (Figure 1F).

754 **Reply:** Thank you. In the submission version, we made a mistake about the number. It
 755 was 0.002-0.05 ppbv instead of 0.1-100 ppbv. We have added the method detection
 756 limit (MDL) for all measured species in Table R2 or Table S4. In Text S1, we have

757 revised "total of 51 VOCs (including 21 alkanes, 13 alkenes, 1 alkyne and 16 aromatics)
758 were analyzed within a limit of quantification of 0.1-100 ppbv" to "total of 51 VOCs
759 (including 21 alkanes, 13 alkenes, 1 alkyne and 16 aromatics) were analyzed within a
760 limit of quantification of 0.002-0.05 ppbv as shown in Table S4".

761

762 **Q34:** Text S2: please define all variables. C_{OH} , t , k , are not defined. Also, Equation S1
763 essentially describes the integrated OH exposure, rather than the "changes in VOC
764 concentration as a function of time due to photochemical reaction".

765 **Reply:** Thank you. We have defined the all variables and revised the description
766 "Equation S1 essentially describes the integrated OH exposure (Shao et al., 2011)" in
767 Text S2 in the revised SI.

768 "Where C_{OH} represents the ambient OH concentration; $k_{A,OH}$ and $k_{B,OH}$ represent the
769 reaction rate of compound A and B with OH radical, respectively; t represents the
770 reaction time of species i in the ambient."

771

772 **Q35:** Table S1: please define all parameters. What's leaf number? Is this the number of
773 leaf nodes, leaf levels/depths, or what? What's fboot?

774 **Reply:** Thank you, we have revised the Table S2 (Table R3). The leaf number represents
775 the minimum number of samples to be split. The fboot represents the minimum number
776 of samples in a leaf. They are added in the footnotes of Table S2.

777

778 Reference

- 779 Breiman, L. Random Forests. *Machine Learning*, 45, 5-32, 10.1023/A:1010933404324, 2001.
- 780 Carter, W.P.L. Development of the SAPRC-07 chemical mechanism. *Atmospheric Environment*, 44,
781 5324-5335, <https://doi.org/10.1016/j.atmosenv.2010.01.026>, 2010.
- 782 Gao, J., Zhang, J., Li, H., Li, L., Xu, L., Zhang, Y., Wang, Z., Wang, X., Zhang, W., Chen, Y., Cheng, X.,
783 Zhang, H., Peng, L., Chai, F., Wei, Y. Comparative study of volatile organic compounds in
784 ambient air using observed mixing ratios and initial mixing ratios taking chemical loss into
785 account – A case study in a typical urban area in Beijing. *Science of The Total Environment*,
786 628-629, 791-804, <https://doi.org/10.1016/j.scitotenv.2018.01.175>, 2018.
- 787 Hou, L., Dai, Q., Song, C., Liu, B., Guo, F., Dai, T., Li, L., Liu, B., Bi, X., Zhang, Y., Feng, Y. Revealing
788 Drivers of Haze Pollution by Explainable Machine Learning. *Environmental Science &*
789 *Technology Letters*, 10.1021/acs.estlett.1c00865, 2022.
- 790 Liu, H., Liu, J., Liu, Y., Ouyang, B., Xiang, S., Yi, K., Tao, S. Analysis of wintertime O3 variability using

791 a random forest model and high-frequency observations in Zhangjiakou—an area with
792 background pollution level of the North China Plain. *Environmental Pollution*, 262, 114191,
793 <https://doi.org/10.1016/j.envpol.2020.114191>, 2020.

794 Liu, Z., Qi, Z., Ni, X., Dong, M., Ma, M., Xue, W., Zhang, Q., Wang, J. How to apply O₃ and PM_{2.5}
795 collaborative control to practical management in China: A study based on meta-analysis and
796 machine learning. *Science of The Total Environment*, 772, 145392,
797 <https://doi.org/10.1016/j.scitotenv.2021.145392>, 2021.

798 Ma, R., Ban, J., Wang, Q., Zhang, Y., Yang, Y., He, M.Z., Li, S., Shi, W., Li, T. Random forest model
799 based fine scale spatiotemporal O₃ trends in the Beijing-Tianjin-Hebei region in China, 2010 to
800 2017. *Environmental Pollution*, 276, 116635, <https://doi.org/10.1016/j.envpol.2021.116635>,
801 2021.

802 Parrish, D.D., Stohl, A., Forster, C., Atlas, E.L., Blake, D.R., Goldan, P.D., Kuster, W.C., de Gouw, J.A.
803 Effects of mixing on evolution of hydrocarbon ratios in the troposphere. *Journal of Geophysical*
804 *Research: Atmospheres*, 112, <https://doi.org/10.1029/2006JD007583>, 2007.

805 Shao, M., Bin, W., Sihua, L., Bin, Y., Ming, W. Effects of Beijing Olympics Control Measures on
806 Reducing Reactive Hydrocarbon Species. *Environmental Science & Technology*, 45, 514-519,
807 [10.1021/es102357t](https://doi.org/10.1021/es102357t), 2011.

808 Wang, T., Xue, L., Brimblecombe, P., Lam, Y.F., Li, L., Zhang, L. Ozone pollution in China: A review of
809 concentrations, meteorological influences, chemical precursors, and effects. *Science of The*
810 *Total Environment*, 575, 1582-1596, <https://doi.org/10.1016/j.scitotenv.2016.10.081>, 2017a.

811 Wang, Y., Li, Y., Pu, W., Wen, K., Shugart, Y.Y., Xiong, M., Jin, L. Random Bits Forest: a Strong
812 Classifier/Regressor for Big Data. *Scientific Reports*, 6, 30086, [10.1038/srep30086](https://doi.org/10.1038/srep30086), 2016.

813 Wang, Y., Wu, G., Deng, L., Tang, Z., Wang, K., Sun, W., Shangguan, Z. Prediction of aboveground
814 grassland biomass on the Loess Plateau, China, using a random forest algorithm. *Scientific*
815 *Reports*, 7, 6940, [10.1038/s41598-017-07197-6](https://doi.org/10.1038/s41598-017-07197-6), 2017b.

816 Yuan, B., Hu, W.W., Shao, M., Wang, M., Chen, W.T., Lu, S.H., Zeng, L.M., Hu, M. VOC emissions,
817 evolutions and contributions to SOA formation at a receptor site in eastern China. *Atmos. Chem.*
818 *Phys.*, 13, 8815-8832, [10.5194/acp-13-8815-2013](https://doi.org/10.5194/acp-13-8815-2013), 2013.

819